L-selectin–mediated Leukocyte Adhesion In Vivo: Microvillous Distribution Determines Tethering Efficiency, But Not Rolling Velocity

By Jens V. Stein,* Guiying Cheng,* Britt M. Stockton,‡ Brian P. Fors,* Eugene C. Butcher,§ and Ulrich H. von Andrian*

*From the *Center for Blood Research and the Department of Pathology, Harvard Medical School, Boston, Massachusetts 02115; and ‡Department of Pathology, Tufts University, Boston, Massachusetts 02111; and the §Laboratory of Immunology and Vascular Biology, Department of Pathology, Stanford University Medical School, Stanford, California 94305; and The Veterans Affairs Palo Alto Health Care Systems, Palo Alto, California 94304*

Summary

Adhesion receptors that are known to initiate contact (tethering) between blood-borne leukocytes and their endothelial counterreceptors are frequently concentrated on the microvilli of leukocytes. Other adhesion molecules are displayed either randomly or preferentially on the planar cell body. To determine whether ultrastructural distribution plays a role during tethering in vivo, we used pre-B cell transfectants expressing L- or E-selectin ectodomains linked to transmembrane/intracellular domains that mediated different surface distribution patterns. We analyzed the frequency and velocity of transfectant rolling in high endothelial venules of peripheral lymph nodes using an intravital microscopy model. Ectodomains on microvilli conferred a higher efficiency at initiating rolling than random distribution which, in turn, was more efficient than preferential expression on the cell body. The role of microvillous presentation was less accentuated in venules below 20 μm in diameter than in larger venules. In the narrow venules, tethering of cells with cell body expression may have been aided by forced margination through collision with erythrocytes. L-selectin transfected cells rolled 10-fold faster than E-selectin transfectants. Interestingly, rolling velocity histograms of cell lines expressing equivalent copy numbers of the same ectodomain were always similar, irrespective of the topographic distribution. Our data indicate that the distribution of adhesion receptors has a dramatic impact on contact initiation between leukocytes and endothelial cells, but does not play a role once rolling has been established.

Key words: selectins • lymphocyte homing • lymph nodes • microvilli • intravital microscopy

Differential expression of a variety of leukocyte adhesion molecules, endothelial counterreceptors, and activating signals constitutes the basis of tissue-specific adhesion (homing) of leukocyte subsets during immune surveillance and inflammation. Thus far, only the selectin family (E-, P-, and L-selectin) and the α4 integrins have been shown to mediate initial contact (tethering) between free-flowing leukocytes and endothelium in vivo. Subsequently, these receptors enable the tethered leukocytes to roll along the vessel wall (1, 2). Rolling leukocytes may adhere firmly by activation-induced interactions of leukocyte integrins with endothelial counterreceptors and transmigrate through the endothelium into the surrounding tissue (1, 2).

The adhesion cascade that mediates homing of lymphocytes to peripheral lymph nodes (PLN)[1] has been elucidated recently on a single cell level (3). Lymphocytes enter specialized subcortical postcapillary venules, called high endothelial venules (HEV), where they tether and roll via L-selectin binding to its endothelial counterreceptor, the peripheral node addressin (PNAd) (3–5), a mixture of sulfated mucin-like sialoglycoproteins defined by the mAb MECA-79 (6, 7). A subset of rolling lymphocytes attaches firmly after ac-

J.V. Stein and G. Cheng contributed equally to this work.

[1]*Abbreviations used in this paper:* BCECF, 2′,7′,-bis-(2-carboxyethyl)-5(and-6) carboxyfluorescein; EC, endothelial cells; ED, ectodomain; HEV, high endothelial venules; LN, lymph node; MFI, mean fluorescence intensity; PLN, peripheral lymph nodes; PNAd, peripheral node addressin; PSGL-1, P-selectin glycoprotein ligand-1; TM/IC, transmembrane and intracellular.

tivation of LFA-1 via a G protein–coupled activation pathway (3) and then transmigrates into the lymph node.

Experiments using neutralizing mAbs or mice that are genetically deficient in L-selectin indicate that L-selectin–dependent tethering and rolling is essential for lymphocyte homing to PLN (8, 9). In vitro studies suggest that this crucial function of L-selectin may be enhanced by its conspicuous surface presentation; L-selectin is preferentially expressed on the tips of microvilli on leukocytes (10, 11), structures long hypothesized to mediate mutual engagement with endothelium (12). Similar to L-selectin, other adhesion molecules capable of mediating tethering such as P-selectin glycoprotein ligand-1 (PSGL-1) and the α4 integrins (primary adhesion receptors) are also targeted to microvilli (13–15). Consequently, the predominance of L-selectin and other primary adhesion receptors on the most distal part of the leukocytes was postulated to facilitate contact with the vessel wall (10–15).

To address this hypothesis, experiments involving domain exchanges between the ectodomain (ED) and the transmembrane and intracellular (TM/IC) domains of L-selectin and CD44 (which is predominantly expressed on the cell body, i.e., excluded from microvilli) have revealed that the TM/IC domains of these proteins determine the spatial distribution of the ED when expressed in the murine pre-B cell line L1-2 (16). In flow chamber assays, L-selectin EDs targeted away from microvilli on the surface of these transfectants were less efficient in initiating tethering to PNAd and mAbs against L-selectin than L-selectin on the tips of microvilli (16).

However, adhesion conditions in vivo differ in several points from those in flow chamber assays. For example, due to the microvascular anatomy, leukocytes are already in close proximity to endothelial cells (EC) upon entry into postcapillary venules and they experience frequent collisions with erythrocytes (17). These physiologic features are thought to promote efficient margination and might render microvillous presentation irrelevant. On the other hand, in vitro studies have shown that microvillous presentation may be increasingly advantageous for tethering when shear rates are increased (16). Leukocytes must tether to EC in vivo in the presence of much higher shear stresses than those employed in vitro (18). Furthermore, electrostatic repulsion between negatively charged glycocalices on the surface of leukocytes (19, 20) and EC (21) may increase the need for exposing adhesion molecules capable of initiating contact on microvilli.

Here, we have taken advantage of the constitutive PNAd expression in PLN to investigate the influence of adhesion receptor distribution in a recently developed intravital microscopy model (5). Our findings confirm that microvillous expression of L-selectin EDs is indeed important for the ability of cells to tether on PLN venules in vivo, and differentiate the role of receptor topography in leukocyte tethering to venules of different diameter. To confirm the importance of adhesion receptor presentation for a pathway not involving L-selectin, we also analyzed the in vivo behavior of L1-2 transfectants expressing wild-type and chimeric E-selectin with different surface distribution, based on the observation that E-selectin can bind to PNAd in vitro (22, 23). Finally, our findings suggest that the distribution of EDs has no influence on the behavior of cells once rolling has been established.

Materials and Methods

Antibodies and Reagents. Anti–human L-selectin mAb DREG-200 (murine IgG1) (24) was purified from hybridoma culture supernatants following standard procedures. Anti–human E-selectin mAb CL-3 (murine IgG1) (25) was generously provided by Dr. C. Wayne Smith (Baylor College of Medicine, Houston, TX). Polyphosphomannan ester (PPME)-FITC was kindly provided by Dr. Lloyd Stoolman (University of Michigan, Ann Arbor, MI). FITC-dextran (150 kD) was purchased from Sigma Chemical Co. Before injection into animals, FITC-dextran was dissolved to 10 mg/ml in sterile saline and centrifuged to remove nonsoluble particles. 2′,7′,-bis-(2-carboxyethyl)-5(and-6) carboxyfluorescein (BCECF; Molecular Probes) was dissolved in DMSO to 0.5 mg/ml and used within 1 wk.

Cell Lines. Murine L1-2 pre-B lymphoma cell lines stably transfected with human wild-type E- and L-selectin have been reported previously (4, 5, 11, 16, 26). The following chimeric L1-2 transfectants, generated by fusing the ED of L- or E-selectin to the TM/IC domain of other surface receptors, have also been described previously (16): L-selectin ED/CD44 TM/IC (L/CD44), and E-selectin ED/L-selectin TM/IC (E/L). L-selectin ED/CD31 TM/IC (L/CD31) was generated in an analogous fashion. In brief, cDNA fragments of the human L-selectin ED and the human CD31 TM/IC domain (a full-length clone was kindly provided by Dr. J. Zehnder, Stanford University, Stanford, CA) (27) were generated by PCR using primers with appropriate overhangs. L/CD31 chimeric cDNA was generated in a second PCR reaction by sequence overlap extension (28). The construct was subcloned in pMRB101 and stably expressed in L1-2 cells following standard procedures. The determination of the surface distribution of the transfected molecules was carried out using low voltage scanning immunoelectron microscopy as described (16). The fusion sites and the surface distribution of the transfected constructs on L1-2 cells are shown in Fig. 1. A parental cell line transfected with the pMRB101 expression vector alone ($L1\text{-}2^{Vector}$) was used as a negative control. L1-2 transfectants were grown in six-well plates in RPMI 1640 containing 10% FCS, standard supplements, 250 μg/ml mycophenolic acid (Sigma Chemical Co.), 12.5 μg/ml xanthine (Sigma Chemical Co.), and 1× hypoxanthine/thymidine (GIBCO BRL).

On the day of an experiment, cells were harvested and counted on a hemocytometer. If >10% dead cells (as determined by Trypan blue exclusion) were present, viable cells were enriched by centrifugation over a Ficoll gradient. Thus, the viability of all cells used in this study was at least 90%. Subsequently, cells were resuspended to 10^7 cells/ml in prewarmed (37°C) RPMI 1640 containing 10% FCS and standard supplements. For fluorescent labeling, cells were incubated for 30 min at 37°C after adding 2.5 μg BCECF/10^7 cells. Labeled cells were washed twice before resuspending them to a final concentration of 1 or 1.5 × 10^7 cells/ml. Aliquots of cells were treated identically, except that no BCECF was added. These samples were then transferred to ice-cold media and stained with mAbs for flow cytometric assessment of receptor expression (see below).

FACS® Analysis. Expression levels of wild-type and chimeric selectins were assessed before and after each experiment.

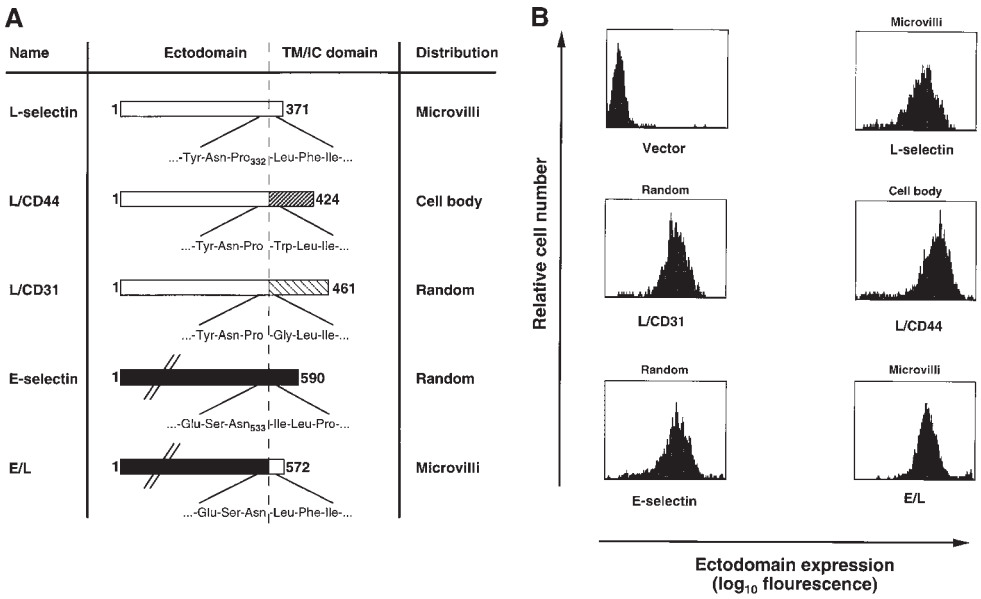

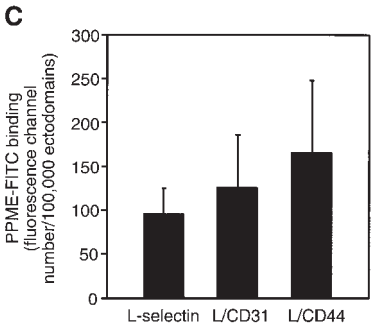

Figure 1. Transfected selectins and their expression in L1-2 cells. (A) Schematic representation of wild-type and chimeric selectins and distribution on L1-2 cells. The predicted number of amino acids (counted from the NH_2 terminus) of each transfected protein is indicated at the left and right of each bar. The amino acid sequence at the splice site is shown with the number of the last amino acid of the ED. The distribution of these molecules on transfected L1-2 cells has been described elsewhere (16), except for L/CD31 (see text). The L-selectin ED and the TM/IC domains were drawn to scale based on their predicted amino acid sequence. The ED of E-selectin is ~60% longer than L-selectin, and was not drawn to scale for clarity (indicated by diagonal lines). (B) Flow cytometry histograms showing typical cell surface expression of wild-type and chimeric selectins. Wild-type L-selectin, L/CD31, and L/CD44 transfectants were stained with anti–human L-selectin mAb DREG-200, as described in Materials and Methods. Wild-type E-selectin and E/L transfectants were stained with anti–human E-selectin mAb CL-3. Staining of mock-transfected L1-2 cells (Vector) with either mAb yielded similar low background fluorescence (shown is staining with DREG-200). (C) PPME-FITC binding to transfectants expressing wild-type or chimeric L-selectin. PPME-FITC binding is expressed as specific MFI per 100,000 L-selectin molecules; data are shown as mean ± SD from four independent experiments.

Transfectants were resuspended in cold PBS containing 1% BSA and 10 μg/ml mAb DREG-200 or mAb CL-3 and incubated for 20 min at 4°C. After washing twice, cells were incubated with PE- or FITC-conjugated goat anti–mouse Ig (Biosource International) for 20 min at 4°C. Cells were washed twice and then analyzed on a FACScan® flow cytometer (Becton Dickinson). L1-2^{Vector} transfectants were stained identically and served as negative control. The mean copy number of wild-type and chimeric ectodomains on transfected cells was estimated using a calibrated microbead system (Quantum Simply Cellular; Flow Cytometry Standards Corp.) following the manufacturer's instructions.

Although all L1-2 transfectants were stably transfected subclones, expression levels varied considerably during culture. Therefore, to allow comparison of cells expressing different receptor topographies, but similar levels of EDs, each transfected cell line was sorted and subcloned. Different subclones were chosen for in vivo experiments when their mean absolute expression levels of selectin EDs were within ±30% of each other and when the nonexpressing population was <10%.

PPME-FITC Binding Assay. PPME-FITC binding assays were carried out as described previously (29). In brief, 10^6 cells were resuspended in 0.2 ml DMEM containing 40 mM Hepes and 10% FBS (assay media) and kept on ice for 30 min in the presence of assay media with or without 25 mM EDTA or 25 μg/ml mAb DREG-200. Subsequently, PPME-FITC was added to all tubes to a final dilution of 1:2,000. After 30 min on ice, samples were directly analyzed by flow cytometry without an additional washing step. The mean fluorescence intensity (MFI) of PPME-FITC labeled cells was determined on a linear fluorescence scale, and specific binding was determined after subtracting the MFI of PPME-FITC in the presence of mAb DREG-200 (background staining). In parallel, the average receptor number per cell was determined using calibrated microbeads as described above. The L-selectin lectin binding activity was expressed as specific fluorescence channel number per 100,000 L-selectin molecules.

Animal Preparation. Mice were anesthetized by i.p. injection of physiologic saline solution containing xylazine (1 mg/ml) and ketamine (5 mg/ml). The left subiliac lymph nodes (LN) of male and female 7–10-wk-old 129SV/C57BL/67 mice (21–23 g) were prepared as described previously (5). In brief, the right femoral artery of each anesthetized mouse was catheterized for retrograde injection of BCECF-labeled cells. Subsequently, the left inguinal fat pad containing the embedded LN was separated from the underlying abdominal wall after a semicircular incision was made in the abdominal skin. The animal was then placed on a custom-made Plexiglas stage, with the skin flap containing the LN spread over a sterile microscope slide, which was constantly kept moist with saline. The fatty tissue covering the embedded LN was carefully removed, avoiding surgical damage to feeding or draining blood vessels.

Intravital Microscopy. Animals were transferred to an intravital microscope (IV-500; Mikron Instruments). Microvessels were

observed through a 10× (Zeiss Achroplan, NA 0.3 ∞) or 20× (Zeiss Achroplan, NA 0.5 ∞) water immersion objective. BCECF-labeled cells were injected through the femoral artery catheter in small boluses of 20–50 μl and visualized in the blood stream by fluorescent epiillumination as described previously (5). The route of cell injection into the inguinal artery which feeds the subiliac LN directly via the superficial epigastric artery allowed us to detect a sufficient number of cells that entered the LN during their first pass through the downstream circulation while keeping the overall number of injected cells low. Thus, when the injection of a cell sample was stopped, the concentration of these cells in the systemic circulation remained low, and very few recirculating cells were found to enter the LN. This allowed us to inject a second sample of transfectants with different ED distribution and to compare the rolling behavior of both cell lines in the same venules. The order in which transfectants were injected was randomized and did not affect their rolling behavior (not shown). We did not attempt to compare more than two cell samples per animal because the number of recirculating cells from previous injections might have become too high to allow a reliable analysis of a third cell sample, and the total volume of injected fluids might have caused unacceptable hemodynamic alterations.

At the end of each experiment, FITC-dextran (150 kD) was injected to visualize the intravascular compartment for measurement of vessel diameters and for determination of venular orders (see below). All scenes were recorded on videotape using a low-lag silicon-intensified target camera (VE1000SIT; Dage MTI), a time base generator (For-A, Co., Ltd.), and a Hi-8 VCR (EVC-100; Sony). At least three independent experiments were carried out for comparison of each pair of transfected L1-2 cells.

Image Analysis. Video analysis was carried out in real time or at reduced speed as described (5, 30). Rolling (i.e., cells that interacted visibly with the endothelium and traveled at a slower velocity than the main blood stream) and noninteracting L1-2 transfectants were counted in each microvessel. The rolling fraction was calculated for each transfectant as percentage of rolling cells among the total number of cells passing a venule during a recorded time interval. Only microvessels with ≥10 cells (total number of cells) were considered for analysis. Included as rolling cells were also cells that displayed jerky motion or skipping behavior. Velocity analysis was carried out by frame by frame analysis of two representative vessels per experiment using a customized image analysis system for microcirculation research (31). For the determination of labeled transfectant velocities, at least 10 consecutive rolling and 20 noninteracting cells were analyzed per vessel and transfectant. V_{roll} was defined as the mean velocity (μm/s) of rolling cells and V_{fast} as the mean velocity of noninteracting cells in each vessel. To correct for hemodynamic differences, V_{roll} was also expressed as percentage of V_{fast} (relative velocity, V_{rel}). For velocity histograms, the velocity of each individual rolling cell was assigned to a velocity class, e.g., from 0 μm/s to <50 μm/s; 50 μm/s to <100 μm/s; and so on, and the frequency of cells in each class was calculated as percentage of all rolling cells analyzed. In addition, a cumulative velocity curve was compiled by plotting the percentage of rolling cells traveling at or below a given velocity as a function of V_{roll}. Rolling fractions and velocities were determined in identical venules for each pair of transfectants, except for comparison of V_{roll} histograms of L1-2 cells expressing wild-type L- and E-selectin, where data from different experiments were pooled. In some cases, the displacements of single fast and rolling cells between two video frames (1/30 s) were measured over up to 25 video frames, and plotted as a function of time.

As described previously, a venular tree in a typical murine PLN consists of one or two collecting venules that receive blood from smaller collecting venules and mid-size medullary venules, which in turn drain small postcapillary venules in the sub- and paracortex (3, 5, 29). Thus, these venules can be subdivided according to their branching order, with terminal collecting venules corresponding to order I, smaller collecting venules and midsize medullary venules to order II or III, and postcapillary venules to order IV or V. Recordings of FITC-dextran–injected preparations were used to determine the venular order and to measure lumenal cross-sectional diameter of blood vessels. From these measurements and the velocity of the fastest noninteracting cells, hemodynamic parameters were calculated as described previously (5, 32).

Statistical Analysis. Data are presented as mean ± SEM unless otherwise indicated. For comparison of rolling fractions of each pair of transfected cells in identical venules, a paired Student's *t* test was employed. For comparison of V_{roll} of each pair of transfectants the Mann-Whitney U test was employed. The Spearman rank correlation test was used for analysis of linear regressions. Statistical significance was set at $P < 0.05$.

Results

Distribution and Expression of Wild-Type and Chimeric L- and E-Selectin on L1-2 Cells. Fig. 1 A shows a schematic representation of transfected selectins. The amino acid sequences at the fusion site between ED and TM/IC domain of chimeric proteins are shown as well. Wild-type and chimeric selectins were previously found to have the following preferential distribution on L1-2 cells, as determined by quantitative analysis of immunogold distribution on labeled cells using low voltage scanning electron microscopy (16): L-selectin and E/L on the tips of microvilli (microvilli: 91 ± 11% and 83 ± 6% of gold particles; cell body: 9 ± 11% and 17 ± 6%, respectively); E-selectin randomly distributed over the entire cell surface (microvilli: 52 ± 8%; cell body: 48 ± 8%); and L/CD44 excluded from microvilli (microvilli: 5 ± 5%; cell body: 95 ± 5%) (16). We confirmed these distribution patterns for the present study (not shown) and also found that L/CD31 is randomly distributed similar to E-selectin (microvilli: 46 ± 8%; cell body: 54 ± 8%) (33 and data not shown).

To assure that ED distribution was the main factor for tethering and rolling ability of the transfected cells (see below), great care was taken to assure equivalent levels of ED expression between L1-2 transfectants. Therefore, L1-2 transfectants were tested before and after each in vivo experiment for comparable expression of EDs by FACS® analysis. Representative histograms are shown in Fig. 1 B. Expression levels of EDs for each pair of transfectants are listed in Table I.

To test whether the TM/IC domain had any influence on the lectin binding activity, binding of lectin domains to PPME-FITC of wild-type and chimeric L-selectin transfectants was determined as described in Materials and Methods. PPME-FITC binding of wild-type and chimeric L-selectin was similar (Fig. 1 C; $P > 0.05$), indicating that the lectin domain retains its functionality in cells expressing chimeric L-selectin.

Table I. *Venular Microhemodynamics in PLN, Rolling Velocities, and ED Expression of L1-2 Transfectants*

	Number of venules/animals	Diameter	V_{fast}	WSR	V_{roll} (median)	V_{rel} (median)	ED expression
		μm	$\mu m/s$	s^{-1}	$\mu m/s$	%	*molecules/cell*
L-selectin	6/3	50.81 ± 9.94	2,519 ± 1,121	417 ± 207	147 ± 114 (99)	5.8 ± 10.2 (4.5)	84,333 ± 34,646
L/CD31			1,765 ± 1,158	352 ± 195	171 ± 111 (148)	9.7 ± 9.6 (8.4)	120,500 ± 29,551
L-selectin	16/4	52.19 ± 21.05	1,685 ± 893	301 ± 216	191 ± 108 (171)	11.3 ± 12.1 (10.1)	116,500 ± 49,950
L/CD44			1,752 ± 951	314 ± 177	216 ± 125 (209)	12.3 ± 13.1 (11.9)	116,330 ± 41,016
L/CD31	8/4	44.03 ± 8.85	970 ± 602	172 ± 82	120 ± 102 (87)	12.4 ± 16.9 (9.0)	182,750 ± 91,350
L/CD44			753 ± 432	148 ± 53	142 ± 88 (121)	18.9 ± 20.4 (16.1)	145,250 ± 59,595
E-selectin	9/3	56.98 ± 13.80	1,453 ± 787	201 ± 83	19 ± 33 (8)	1.3 ± 4.2 (0.6)	97,500 ± 45,962
E/L			1,916 ± 1,079	254 ± 95	20 ± 28 (11)	1.0 ± 2.6 (0.6)	75,500 ± 20,506

Mean velocities of noninteracting (V_{fast}) and rolling L1-2 transfectants (V_{roll}) were measured in at least two representative venules per animal. These data combined with the venular diameter were used to calculate the wall shear rate and wall shear stress as described in Materials and Methods. To correct for hemodynamic differences between subsequent observations of pairs of transfectants, V_{roll} was also expressed as percentage of V_{fast} (V_{rel}). The average receptor number per cell was assessed for each transfectant on the day of an experiment as described in Materials and Methods. All data are presented as mean ± SD.

Behavior of Wild-Type and Chimeric L-Selectin Transfectants in Subiliac PLN. BCECF-labeled transfectants were injected through the femoral artery and observed in subiliac PLN microvessels. These vessels are classified in up to five branching orders in a typical nodal venular tree as described previously (3, 5). In agreement with previous studies of L1-2 transfectants expressing wild-type L-selectin, we found that their rolling fraction was highest in immediate postcapillary venules (orders IV and V), gradually decreasing in successively larger venules downstream (orders III to I) (5). This decrease in rolling fractions was shown to correlate with a decrease in PNAd density (29). Accordingly, we found a similar spatial preference in rolling for chimeric L-selectin transfectants (Fig. 2, A–C); irrespective of the ultrastructural distribution of L-selectin EDs, all cell lines rolled consistently more frequently in high order venules where L-selectin ligands were abundant, and displayed much less rolling in medullary collecting venules with sparse PNAd expression. Tethering and rolling was mediated by the EDs of transfected selectins as mock-transfected L1-2 cells were not able to tether and roll in this model (5). In agreement with previous studies with L1-2 transfectants in murine PLN, we did not observe transfectants that became stuck (stationary for ≥30 s) in any postcapillary venule analyzed, probably because these cells express very few β2 integrins which are necessary for firm adhesion in PLN HEV (3, 5).

L-Selectin Tethering Efficiency In Vivo Depends on ED Surface Distribution. To investigate the influence of receptor distribution on the cell surface, we determined the rolling fraction of pairs of transfectants that were injected at random order in the same animal. The rolling fraction strongly depended on the topography of L-selectin. L1-2 cells expressing wild-type L-selectin EDs that were located preferentially on microvilli rolled more frequently than those that were randomly distributed (L/CD31) or concentrated on the cell body (L/CD44). L/CD31 receptors were more efficient than L/CD44 EDs (Fig. 2, A–C).

Although venules in all LN preparations supported significant rolling of L1-2 transfectants, there was considerable heterogeneity between individual experiments and between series of experiments that were performed during different periods of time (compare rolling fractions of wild-type L-selectin transfectants in Fig. 2 A and Fig. 2 B). However, irrespective of the baseline adhesiveness of the endothelial substrate, the ability of L1-2 transfectants to engage in rolling invariably followed a topographic hierarchy: microvillous > random > cell body presentation. To establish this relationship, we compared cell lines in a pairwise fashion, injecting one after another in the same animal, and then calculated the relative rolling fraction for each pair of transfectants in each venule. For this, the rolling fraction of the cell line that displayed an overall lower frequency of rolling was normalized to the rolling fraction of the other cell line (Fig. 2 D). We found that wild-type L-selectin was on average 1.87 ± 0.19 (mean ± SEM) times more efficient at initiating interactions with PNAd than L/CD31 and 2.70 ± 0.22 times more efficient than L/CD44. In turn, 1.63 ± 0.12 times more L/CD31 transfectants rolled in LN venules compared with L/CD44 cells. This reveals an incremental loss of tethering efficiency in vivo as EDs are redistributed away from the tips of microvilli.

Microvillous Distribution of L-Selectin Is Most Important in Venules of >20 μm Diameter. Lymphocyte–EC interactions in PLN take place mostly in immediate postcapillary venules (diameter 10–20 μm) and venules created by merging of these postcapillary venules (diameter >20 μm). To test whether microvillous exposure of L-selectin is more important in one or the other, we analyzed the role of receptor distribution on L-selectin and L/CD44 trans-

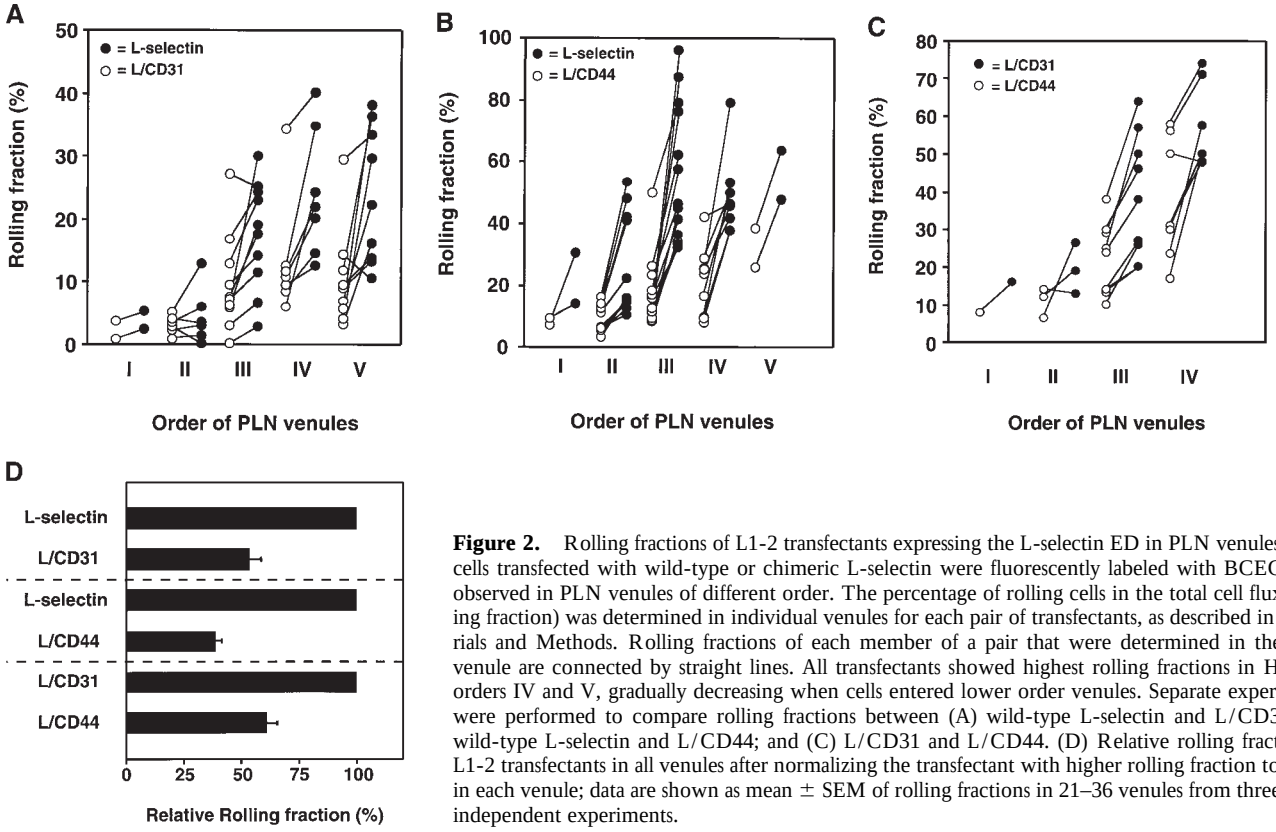

Figure 2. Rolling fractions of L1-2 transfectants expressing the L-selectin ED in PLN venules. L1-2 cells transfected with wild-type or chimeric L-selectin were fluorescently labeled with BCECF and observed in PLN venules of different order. The percentage of rolling cells in the total cell flux (rolling fraction) was determined in individual venules for each pair of transfectants, as described in Materials and Methods. Rolling fractions of each member of a pair that were determined in the same venule are connected by straight lines. All transfectants showed highest rolling fractions in HEV of orders IV and V, gradually decreasing when cells entered lower order venules. Separate experiments were performed to compare rolling fractions between (A) wild-type L-selectin and L/CD31; (B) wild-type L-selectin and L/CD44; and (C) L/CD31 and L/CD44. (D) Relative rolling fraction of L1-2 transfectants in all venules after normalizing the transfectant with higher rolling fraction to 100% in each venule; data are shown as mean ± SEM of rolling fractions in 21–36 venules from three to six independent experiments.

fectants in vessels of different diameters. The relative advantage of microvillous ED presentation in vessels of increasing diameter was expressed as the ratio of the rolling fractions of both transfectants in each individual venule (Fig. 3). On average, 2.5 times more microvillous transfectants than cell body transfectants rolled in the smallest venules (10–20 μm diameter), whereas this ratio was increased to 4.2 in vessels of twice that diameter (20–40 μm). Indeed, there was a statistically significant linear correlation between the relative advantage of microvillous transfectants to initiate interactions in PLN venules and the diameter of these venules (Spearman rank correlation test: $P < 0.05$).

L1-2 Cells Expressing Human E-Selectin Acquire the Ability to Roll in PLN Venules. The results presented above are strongly suggestive of a pivotal role of surface distribution for L-selectin–dependent rolling. However, theoretically it remained possible that the replacement of TM/IC domains in the two mutants had conferred a distribution-independent disadvantage in tethering efficiency relative to wild-type L-selectin. For instance, a conformational change in the chimeric molecules could have altered the orientation of the lectin domain that might have affected its ability to bind surface-bound ligands (such as PNAd), but not freely diffusible ligands (such as PPME-FITC). Therefore, we sought to corroborate our findings using a molecularly distinct adhesion pathway that could be tested in our in vivo system.

An earlier study has reported that E-selectin/IgG chimeric molecules bind to PNAd in HEV in frozen sections of murine PLN and human tonsils (22), and E-selectin–transfected cells were shown to bind to immobilized PNAd (23). Thus, we tested whether L1-2 cells expressing human E-selectin could interact with subiliac LN venules. Indeed, cells expressing E-selectin EDs tethered and rolled in PLN HEV similar to L-selectin transfectants, i.e., rolling fractions were highest in order IV and V venules, and decreased in lower order venules (Fig. 4 A).

E-Selectin–mediated Rolling Is Slower than Rolling Via L-Selectin, But Surface Distribution Is Equally Important for Tethering. In almost all venules analyzed, E/L on microvilli

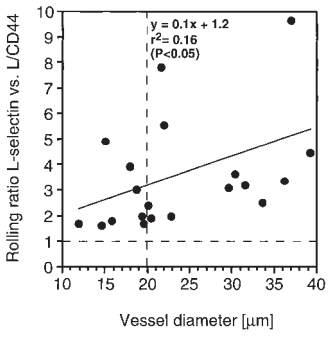

Figure 3. Microvillous expression of L-selectin confers enhanced tethering in all venules, but is most critical in venules with diameters above 20 μm. Rolling fractions were determined as described in Materials and Methods. The ratio of rolling fractions of wild-type L-selectin (microvillous) versus L/CD44 (cell body) transfectants was determined for venules with different diameters. Each point represents one venule. A ratio of one (hatched horizontal line) indicates equal rolling fractions, a ratio of two means that wild-type transfectants rolled twice as frequently in a venule than L/CD44 cells, and so on. A linear regression line was generated with the help of PC-based graphics software (Sigma Plot). Note that rolling ratios in many venules with diameters below 20 μm (indicated by vertical broken line) tend to be lower than in larger vessels.

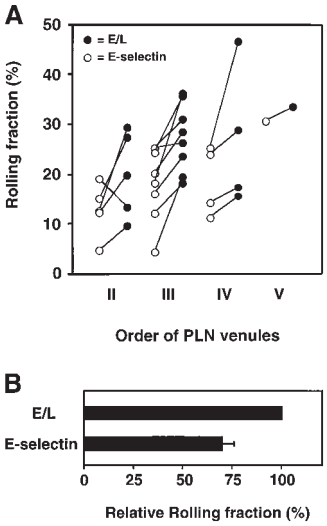

Figure 4. Rolling fractions of L1-2 cells expressing the E-selectin ED in PLN venules. Rolling fractions in PLN venules of transfectants expressing E-selectin (random distribution) and E/L chimera (on microvilli) are presented as in Fig. 2. (A) Rolling fractions of E/L and wild-type E-selectin transfectants in paired venules. (B) Relative rolling fraction determined by normalizing the rolling fraction of E-selectin transfectants to that of E/L transfectants in each venule; data are shown as mean ± SEM of rolling fractions in 18 venules from three independent experiments.

conferred higher rolling fractions than randomly distributed E-selectin (Fig. 4 A). The relative rolling fraction of E/L transfectants was 1.43 ± 0.12 times higher than that of wild-type E-selectin transfectants (Fig. 4 B).

Interestingly, cells transfected with E-selectin EDs rolled at much slower velocities than wild-type L-selectin transfectants (Fig. 5, A and B) despite comparable ED expression numbers and hemodynamic conditions (Table I). Approximately 95% of E-selectin transfectants rolled slower than 50 μm/s, whereas only 9.6% of L-selectin transfectants were found in this velocity class. The average (± SEM) V_{roll} in all venules combined was 19 μm/s ± 3.8 for wild-type E-selectin transfectants (n = 73 cells/9 venules/3 experiments) and 181 ± 6.9 μm/s (n = 260/22/7) for wild-type L-selectin transfectants.

Rolling Velocity Is Independent of Receptor Distribution. To determine the role of ED distribution on V_{roll}, we carried out a detailed analysis of single cell rolling velocities for each pair of transfectants. Chimeric transfectants expressing the L-selectin ectodomain showed similar average V_{roll} when compared to their wild-type or other chimeric counterparts (Table I). For further analysis of L1-2 cell rolling behavior in PLN HEV, velocity histograms and cumulative velocity curves were calculated as shown in Fig. 5. The velocity histograms of pairs of cell lines tested in the same preparation were comparable between all L-selectin transfectants (Fig. 6, A, C, and E). Accordingly, the cumulative velocity curves (Fig. 6, B, D, and F) were nearly superimposable. Likewise, E/L and wild-type E-selectin transfectants were found to have similar velocity histograms and cumulative velocity curves (Fig. 6, G and H). A statistical comparison of the medians of the L/CD31-L/CD44 pair, but not of any other pair, revealed a significant difference (Mann-Whitney U test; $P < 0.05$). The low V_{roll} of L/CD31 cells in this group may have been due to their unusually high expression of L-selectin EDs and relatively low shear rates (Table I). No significant differences were found in V_{roll} or V_{rel} with L/CD31 transfectants that expressed lower ED levels during comparison with wild-type L-selectin transfectants.

To detect subtle alterations in rolling behavior that might remain unnoticed during measuring V_{roll} over a long distance, we also analyzed the displacement of rolling and noninteracting L-selectin and L/CD44 transfectants from one video frame to the next (i.e., every 1/30 s) in identical venules (Fig. 7, A and B). We were not able to detect qualitative differences in the rolling behavior of cells displaying L-selectin on the microvilli or on the cell body. Both cell types displayed a jerky rolling motion characterized by frequent shifts in V_{roll} and brief hesitations that is also typical for L-selectin–dependent rolling on PNAd in vitro (34).

Discussion

We have used murine pre-B cells transfected with wild-type or chimeric L-selectin and E-selectin to assess the influence of adhesion receptor topography on rolling behavior in vivo. We took advantage of a recently developed model of intravital video microscopy to study the passage

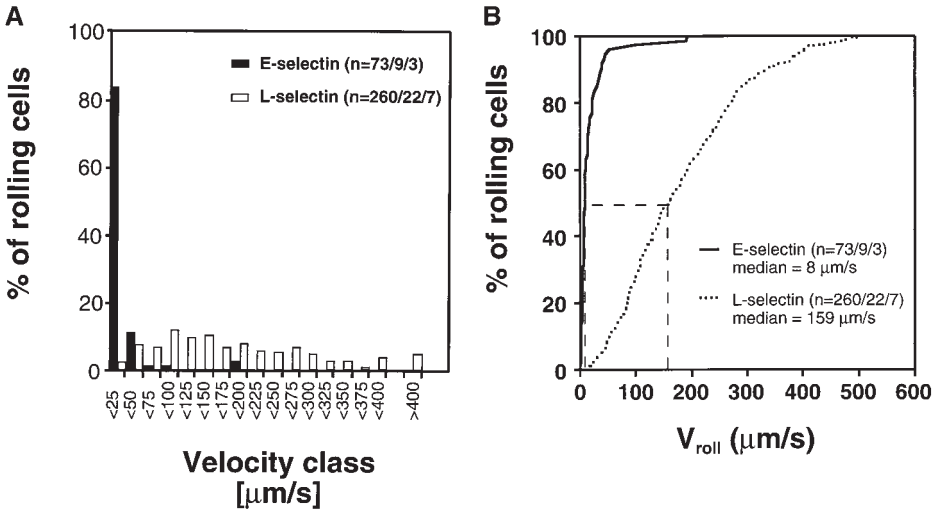

Figure 5. E-selectin transfectants mediate slower rolling than L-selectin transfectants. (A) A velocity histogram was generated by measuring rolling velocities of individual cells in PLN venules as described in Materials and Methods. Frequency distributions were calculated after cells were assigned to velocity classes from >0 μm/s to <25 μm/s; 25 to <50 μm/s; and so on. (B) Cumulative velocity curves of E- and L-selectin transfectants. The percentage of rolling cells is expressed as a function of V_{roll} (see Materials and Methods). n = number of cells/venules/experiments analyzed.

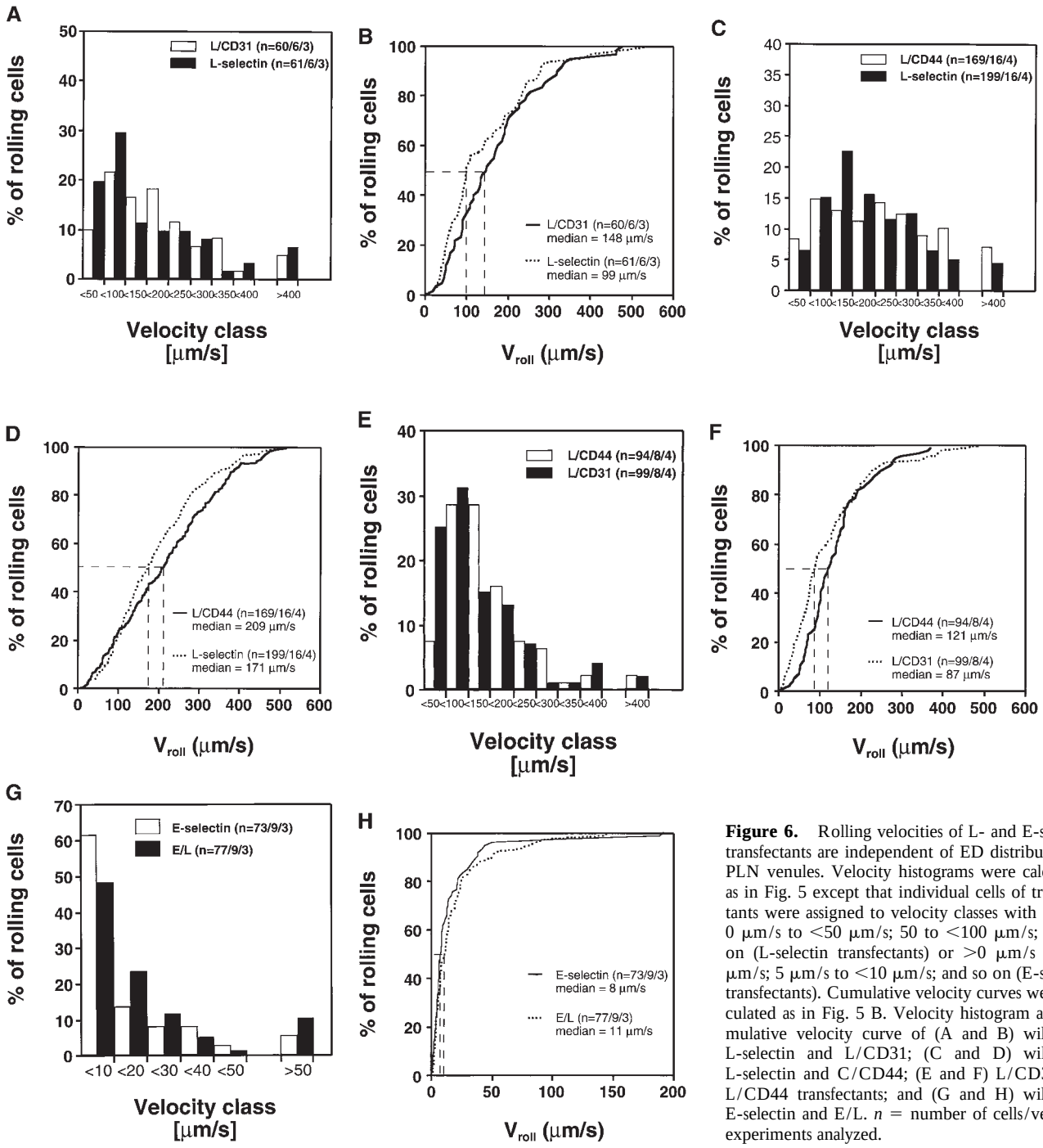

Figure 6. Rolling velocities of L- and E-selectin transfectants are independent of ED distribution in PLN venules. Velocity histograms were calculated as in Fig. 5 except that individual cells of transfectants were assigned to velocity classes with $V_{roll} >$ 0 μm/s to <50 μm/s; 50 to <100 μm/s; and so on (L-selectin transfectants) or >0 μm/s to <5 μm/s; 5 μm/s to <10 μm/s; and so on (E-selectin transfectants). Cumulative velocity curves were calculated as in Fig. 5 B. Velocity histogram and cumulative velocity curve of (A and B) wild-type L-selectin and L/CD31; (C and D) wild-type L-selectin and C/CD44; (E and F) L/CD31 and L/CD44 transfectants; and (G and H) wild-type E-selectin and E/L. *n* = number of cells/venules/experiments analyzed.

of fluorescently labeled cells through subiliac lymph nodes (5). We chose the PLN model rather than other intravital microscopy models because of the constitutive PNAd expression in lymph node vessels (6, 29), which supports reproducible rolling interactions of L-selectin transfectants at a much higher frequency than nonlymphoid tissues such as the mesentery (5, 26, 35).

Our results demonstrate that (a) the ultrastructural surface distribution of primary adhesion receptors has a strong impact on the ability of transfectants to initiate adhesion to EC; (b) the relative advantage of microvillous versus cell body presentation is most accentuated in venules of 20–40 μm diameter; (c) E-selectin transfectants roll significantly more slowly than L-selectin transfectants, presumably interacting with the same substrate, PNAd, under comparable hemodynamic conditions; and (d) once transfectants begin to roll on EC, the rolling velocity is independent of receptor distribution.

Using a flow assay in which transfectants were perfused through ligand-coated glass capillaries, we have shown pre-

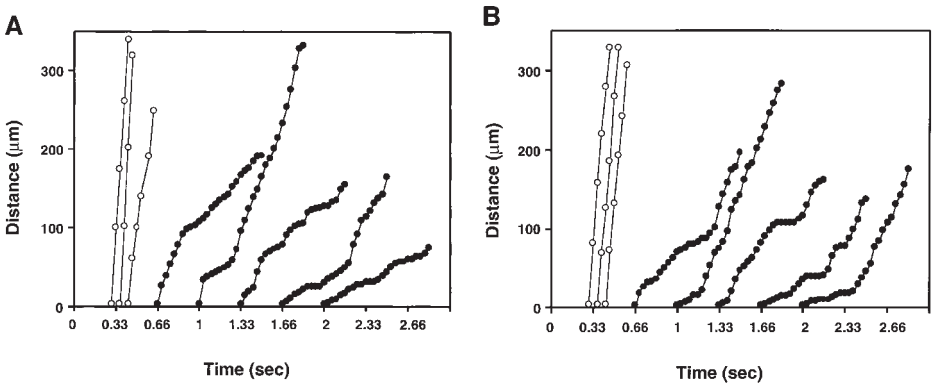

Figure 7. Similar rolling behavior of cells displaying L-selectin on the microvilli or on the cell body. The distance traveled between two video frames (1/30 s) was determined for five randomly chosen rolling cells (filled circles) and three fast cells (open circles) in the same venule (×20 lens). The y-axis indicates the length (in μm) traveled, with zero as the upstream entry point into the venule. Symbols connected by lines indicate the relative position of a cell at each of up to 25 consecutive video frames. The time at which the cells enter the field of view is arbitrary. (A) L-selectin transfectants; (B) L/CD44 transfectants.

viously that microvillous expression of L-selectin allows transfectants to initiate interactions with purified PNAd or immobilized anti–L-selectin mAb more efficiently than cell body expression of the same ED (16). However, tethering in vivo occurs under much higher shear rates than possible in flow chamber assays (18). Furthermore, ligand densities are likely to differ under in vivo and in vitro conditions. The negative charge associated with the glycocalyx of leukocytes (19, 20) and EC (21) generating electrostatic repulsion might also be different in vivo compared to in vitro assays. In addition, most flow chamber assays rely on gravity to allow horizontally perfused leukocytes to collide with the substrate-coated floor of the chamber, whereas the influence of gravitational forces is negligible for leukocyte margination in vivo. Instead, blood-borne leukocytes are forced into the proximity of ECs by anatomical constraints (e.g., in capillaries) or by collision with other blood cells, particularly erythrocytes (17). These physiologic factors are difficult to reproduce in vitro, although one study has reported increased leukocyte–EC interactions after infusing red blood cells into a flow chamber (36). Therefore, it has been unclear whether and to what extent adhesion receptor presentation on microvilli is necessary for contact formation between free-flowing leukocytes and EC under physiologic conditions. Here we show that microvillous presentation of L-selectin conferred a much higher tethering capability compared with cell body presentation (L/CD44) and with randomly distributed adhesion receptors (L/CD31) in almost all venules analyzed. Furthermore, we also observed an advantage of randomly distributed L/CD31 over microvillous-excluded L/CD44.

Interestingly, there was no significant correlation between the wall shear rate and the rolling ratio of L-selectin versus L/CD44 transfectants (not shown). This is in contrast to in vitro findings, where the importance of microvillous L-selectin was much more pronounced at higher shear rates (16). This apparent difference between in vivo and in vitro experiments underscores the importance of collisions between leukocytes and erythrocytes in venules, which have been shown to be the principal mechanism of leukocyte margination at high shear (17, 36). As shear rates increase, the duration of contacts with the endothelium will be shortened, leading to a reduced likelihood of tether formation, especially for nonmicrovillous receptors. However, at the same time collisions with RBCs are likely to become more frequent and more forceful, thus allowing more flexing of microvilli and enhanced exposure of cell body receptors. These two opposing mechanisms may cancel each other out, resulting in an overall constant role for microvillous receptor topography over a wide range of shear rates.

However, we found that the relative advantage of microvillous versus cell body presentation of L-selectin EDs was most accentuated in venules with diameters of >20 μm, whereas postcapillary venules with diameters <20 μm supported tethering of cell body transfectants that was relatively more frequent, yet still lower than observed for wild-type transfectants. This attenuated effect in very small HEV might be explained by a forced margination phenomenon that occurs preferentially in immediate postcapillary venules (17). When a leukocyte (or L1-2 cell) encounters the capillary bed, its cellular diameter frequently exceeds the diameter of the capillary ostium. Therefore, the cell is forced to deform itself (37) before it can be squeezed through the narrow capillary. During the ensuing brief delay, blood plasma flows around the slow moving cell resulting in a cell-free plasma gap downstream of the leukocyte while erythrocytes pile up behind its trailing end (17). After entering wider postcapillary venules, the stiff and large leukocyte still experiences considerable drag, even in the absence of adhesive interactions. The smaller and highly deformable erythrocytes that have accumulated behind the leukocyte in the capillary now have sufficient space to pass the leukocyte and push it against the venular endothelium. This phenomenon might cause some flexing of microvilli and, thus, might enhance the accessibility of L-selectin EDs located on the cell body. However, this effect may fade as leukocytes pass into postcapillary vessels of larger diameter where erythrocyte-induced margination may be less forceful (Fig. 8). In addition, the endothelial wall of HEV bulges out into the luminal space of postcapillary venules (orders IV and V), thus increasing the probability of leukocyte–EC collisions (5). On the other hand, the endothelial lining of larger venules (orders III and lower) is more flattened (38), which might enhance the need for exposing L-selectin to

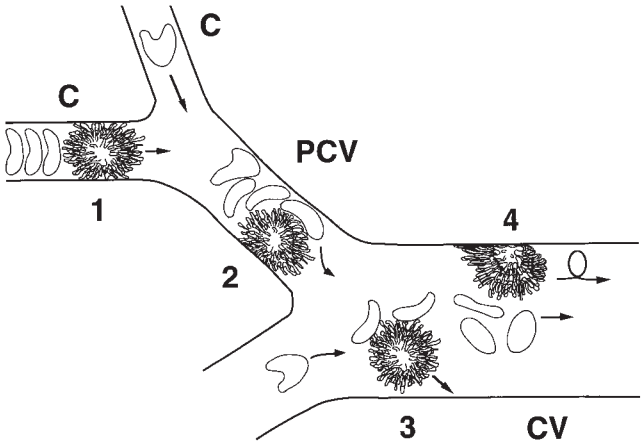

Figure 8. A differential role for microvillous receptor presentation in PLN microvessels of different sizes. (1) RBCs pile up behind slower moving leukocytes in narrow capillaries (C, diameter 5–10 μm). As capillary ECs are not adhesive, there is no apparent binding despite the close proximity between cell membranes. (2) When entering the smallest postcapillary venules (PCV, diameter 10–20 μm), RBCs pass through the gap between the leukocyte and the venular wall and push the slow moving leukocyte against endothelial counterreceptors. This may promote contact initiation between leukocytes and EC (forced margination [17]). In this process, microvilli may be flexed, leading to exposure of some nonmicrovillous receptors. (3) In larger postcapillary and collecting venules (CV, diameter >20 μm), leukocytes experience little drag and move at a similar velocity as erythrocytes. Thus, collisions with RBCs might be less forceful, thereby enhancing the need of microvillous presentation of adhesion receptors to contact EC counterreceptors. (4) Once rolling has been established, the cell surface distribution of adhesion receptors mediating rolling does not seem to be important as leukocytes are pushed against the venular wall and become flattened to allow receptors located on any part of the cell surface to interact with endothelial counterreceptors.

initiate contact with endothelial counterreceptors. Taken together, these factors might explain the increasing tethering advantage of microvillous L-selectin with increasing diameter. Thus, our findings highlight the different conditions encountered during in vivo and in vitro assays; whereas the differential effect of microvillous versus cell body presentation was shown in vitro to be a function of shear (16), we find that this effect is a function of the vessel diameter in vivo.

Our data also show that E-selectin transfectants were able to tether and roll in PLN venules. E-selectin/Ig chimera has been reported previously to recognize HEV in immunohistochemical stainings (22). Furthermore, E-selectin has been shown to bind to PNAd coated on glass slides (23). Although E-selectin is normally only expressed on EC (39), the transfectants used in this study are a useful model to investigate the impact of differential receptor topography on tethering efficiency using an adhesion pathway that does not involve L-selectin. Analogous to wild-type L-selectin and L/CD31, we found that microvillous E/L conferred higher tethering efficiency compared to randomly distributed E-selectin. Thus, the ability of adhesion receptors to initiate interactions with their ligands under physiologic conditions is dependent on their surface distribution; microvillous, i.e., most distally positioned EDs, are more efficient than randomly distributed ones, which in turn are more efficient than cell body expressed receptors.

It might be argued that the TM/IC domains influenced the ability of EDs to bind to their ligands in some other way, e.g., by altering the structure or function of the ED. However, all transfected cell lines displaying L-selectin EDs were shown to bind PPME-FITC similarly. This shows that the lectin domain of L-selectin involved in binding to endothelial counterreceptors remained unaffected by the (chimeric) nature of its TM/IC domain. Due to the lack of an appropriate reagent, we were not able to test the lectin binding activity of wild-type and chimeric E-selectin. However, E/L and wild-type E-selectin transfectants rolled at equivalent velocities suggesting that the lectin activity of chimeric E-selectin remained unaffected by its TM/IC domain. Moreover, domain swapping in E/L cells resulted in a gain of function, i.e., enhanced tethering efficiency of chimeric over wild-type transfectants. This indicates that the effects of replacing TM/IC domains on the tethering ability of selectin EDs are most likely due to changes in topographic distribution and not altered ED conformation.

Our experiments do not exclude the possibility that the cytoskeletal association was different between wild-type and chimeric molecules. Indeed, it is likely that differential interactions of TM/IC domains with domain-specific cytoskeletal components were responsible for the observed topographic specificities. However, it appears probable that each of the molecules expressed in L1-2 cells was anchored sufficiently. It has been reported that transfectants expressing truncated L-selectin that lacked most of the intracellular domain and no longer appeared to be linked to the cytoskeleton failed to bind endothelial counterreceptors in vitro and in vivo (40). Moreover, disruption of the actin-based cytoskeleton with cytochalasin B or D was found to greatly reduce the tethering efficiency of cell lines transfected with L-selectin and of human neutrophils (16, 40, 41). The finding that the transfectants used here retained a certain capacity to initiate rolling and the observation that V_{roll} was equivalent between cells with the same ED indicates that the cell lines used in this study presented their transfected adhesion molecules sufficiently anchored in the cell membrane. Thus, the cell surface distribution pattern conferred by TM/IC domains is likely to be the main factor in determining the ability of transfected cells to tether to the endothelium.

It cannot be excluded that intracellular signaling via TM/IC domains may be altered in chimeric proteins. However, contact initiation between free-flowing lymphocytes and endothelium is a nearly immediate process that is unlikely to require prior signaling. However, it is conceivable that downstream signaling events initiated by primary adhesion receptors may be triggered by their engagement in rolling interactions. In circulating lymphocytes which rely on L-selectin to initiate adhesive contact when they home to PLN, such early events could contribute at later stages, such as during firm arrest and transmigration (3, 42, 43).

Most other adhesion receptors capable of initiating contact with EC under flow are also targeted to the tips of microvilli, such as PSGL-1 (13) and the α4 integrins (14, 15).

In addition, the cutaneous lymphocyte antigen, an sLex-like carbohydrate determinant on myeloid and lymphoid cells which mediates binding to E-selectin, has been reported to be associated with PSGL-1 (44). Therefore, it is likely that at least some E-selectin ligands are also preferentially expressed on the tips of microvilli. These findings, combined with our data, support the hypothesis that white blood cells optimize their recruitment by exposing the molecules that initiate adhesion on the most distal parts of their surface. On the other hand, secondary adhesion receptors mediating firm adhesion after rolling, such as β2 integrins, are found on the cell body (10).

Other adhesion molecules, such as E-selectin ligand-1 or CD44, are targeted to the side of microvilli (45) or to the cell body, respectively (16). Both can mediate some degree of adhesion on their respective ligands in vitro (46, 47). However, their role in initiating contact with EC in vivo is unclear. Conceivably, these receptors may participate primarily in the strengthening of rolling once contact has been initiated by other adhesion molecules on the tips of microvilli. On the other hand, our data show that randomly or microvilli-excluded EDs are also able to initiate contact under physiologic conditions, albeit much less efficiently than EDs on the tips of microvilli.

E-selectin transfectants rolled considerably more slowly (~10-fold) than L-selectin transfectants. All selectins bind to composite ligands containing sLex-like carbohydrate structures (48). Both L- and E-selectin can recognize PNAd (23), but their binding sites may not be identical (22). For example, L-selectin binding to human and murine HEV using immunohistochemical methods can be blocked by fucoidan, but remains unaffected by soluble sLex, whereas the opposite is the case for E-selectin (22). Furthermore, L-selectin requires sulfated ligands under physiologic conditions (7), whereas E-selectin may not (47). Thus, it cannot be excluded that the ligand density in HEV was much higher for E-selectin in HEV than for L-selectin, which may have contributed to the differences in V_{roll}. However, L-selectin ligands are abundantly expressed in PLN, in particular in high order HEV (29). Moreover, there was no detectable difference in V_{roll} between high and low order venules (not shown). Thus, it seems unlikely that the density of L-selectin ligands on HEV was a limiting factor that influenced the rolling velocity of cells expressing the L-selectin EDs. In addition, neutrophils have been found to roll 8–11.5-fold faster on the L-selectin ligand CD34 than on E-selectin in flow chamber assays when both substrates were used at comparable site densities (49). We found a similar ratio using cells expressing similar numbers of L- or E-selectin ED under comparable physiologic conditions. Therefore, it is likely that intrinsic differences in the bond lifetime, with E-selectin having a much longer bond lifetime compared to L-selectin (49), are responsible for the slower rolling of E-selectin transfectants.

It has been suggested in several theoretical models of leukocyte rolling that the spacing between adhesion receptors on the tips of microvilli engaged in interactions with EC counterreceptors plays a role in determining the velocity of rolling leukocytes (50, 51). To address this question, we assessed the influence of cell surface distribution of L- and E-selectin on V_{roll} and V_{rel}. Hemodynamic parameters were comparable for each pair of transfectants tested, although the average V_{fast} was somewhat lower for the comparison of L/CD31 and L/CD44 transfectants than for the other pairs, reflecting random variability between preparations.

Our analysis revealed that the rolling velocity is independent of receptor topography for each pair of transfectants investigated. It is conceivable that microvilli constitute flexible structures that may quickly adapt to forces exerted by the flowing blood (Fig. 8). Indeed, previous in vivo studies suggest that rolling leukocytes become flattened as they are pushed against ECs by the flowing blood (18). Thus, our in vivo findings do not agree with theoretical models of leukocyte rolling where microvilli are assumed to be rigid structures whose spacing determines the distance between successive adhesion events in flow direction mediated by microvillous receptors, thereby determining the rolling velocity at a given flow rate (50, 51). Several factors might explain these differences. First, the torque acting on a rolling leukocyte under shear can be divided in two perpendicular force vectors, one acting in the direction of flow, the other normal to the endothelium (34). The higher the shear stress, the more leukocytes are pushed against EC by the normal force, thereby they are forced to flatten (18). Second, RBCs colliding with rolling leukocytes might push leukocytes further against the endothelium. Third, the trailing end of a rolling cell experiences most of the tensile force that pulls transmembrane receptors. This may lead to stretching of the downstream plasma membrane in the area of contact with the vascular wall and cause flattening or retraction of microvilli. However, it must be noted that cell flattening does not necessarily mean that microvilli are not present at the contact surface between leukocytes and ECs. Alternatively, they might be pushed aside, with the adhesion receptors on the trailing edge conferring the necessary contact to the endothelial counterreceptors. In any event, the structural changes in the contact zone between the rolling cell and the venular endothelium appear to allow receptors on all microdomains (i.e., microvillous and nonmicrovillous) to contribute to the overall strength of the interaction. This would explain the congruence of V_{roll} that was observed to occur between cells that express adhesion molecules on different surface domains while in suspension, and might enable adhesion receptors on other parts of the cell, such as β2 integrins on the cell body, to interact with EC counterreceptors.

In conclusion, we have demonstrated that the surface distribution of leukocyte adhesion receptors plays a critical role in initiating contact between circulating leukocytes and endothelial ligands under physiologic conditions. We confirm data from previous in vitro assays showing that presentation of L-selectin on the surface of leukocytes has a dramatic impact on tethering efficiency and we expand the data to the in vivo situation. Furthermore, our data suggest a differential advantage of microvillous presentation

of L-selectin in vivo that is inversely correlated with the venular diameter, but does not seem to be correlated with the shear forces. Our findings also reveal that topography is important for tethering but it does not influence the strength of established rolling interactions. These observations support the hypothesis that exposed presentation of primary adhesion receptors increases interactions between leukocytes and endothelium in vivo and constitute an additional refinement of the multistep adhesion cascade.

We would like to thank Dr. E. Quackenbush for critical reading of the manuscript, Mark Ryan for valuable help with FACS® sorting, as well as Drs. C. Wayne Smith, Lloyd Stoolman, and James Zehnder for mAb CL-3, PPME-FITC, and for CD31 cDNA, respectively.

This work was supported by National Institutes of Health grant HL54936.

This study complies with NIH guidelines and was approved by the Institutional Review Committees on Animals of both Harvard Medical School and CBR. Animals were under complete surgical anesthesia throughout all experimental procedures.

Address correspondence to Ulrich H. von Andrian, The Center for Blood Research, Harvard Medical School, 200 Longwood Ave., Boston, MA 02115. Phone: 617-278-3130; Fax: 617-278-3190; E-mail: uva@cbr.med.harvard.edu

Received for publication 16 July 1998 and in revised form 27 October 1998.

References

1. Salmi, M., and S. Jalkanen. 1997. How do lymphocytes know where to go: current concepts and enigmas of lymphocyte homing. *Adv. Immunol.* 64:139–218.
2. Butcher, E.C., and L.J. Picker. 1996. Lymphocyte homing and homeostasis. *Science.* 272:60–66.
3. Warnock, R.A., S. Askari, E.C. Butcher, and U.H. von Andrian. 1998. Molecular mechanisms of lymphocyte homing to peripheral lymph nodes. *J. Exp. Med.* 187:205–216.
4. Berg, E.L., M.K. Robinson, R.A. Warnock, and E.C. Butcher. 1991. The human peripheral lymph node vascular addressin is a ligand for LECAM-1, the peripheral lymph node homing receptor. *J. Cell Biol.* 114:343–349.
5. von Andrian, U.H. 1996. Intravital microscopy of the peripheral lymph node microcirculation in mice. *Microcirculation.* 3:287–300.
6. Streeter, P.R., B.T.N. Rouse, and E.C. Butcher. 1988. Immunohistologic and functional characterization of a vascular addressin involved in lymphocyte homing into peripheral lymph nodes. *J. Cell Biol.* 107:1853–1862.
7. Hemmerich, S., E.C. Butcher, and S.D. Rosen. 1994. Sulfation-dependent recognition of high endothelial venules (HEV)-ligands by L-selectin and MECA 79. *J. Exp. Med.* 180:2219–2226.
8. Arbonès, M.L., D.C. Ord, K. Ley, H. Ratech, C. Maynard-Curry, G. Otten, D.J. Capon, and T.F. Tedder. 1994. Lymphocyte homing and leukocyte rolling and migration are impaired in L-selectin–deficient mice. *Immunity.* 1:247–260.
9. Gallatin, W.M., I.L. Weissman, and E.C. Butcher. 1983. A cell-surface molecule involved in organ-specific homing of lymphocytes. *Nature.* 304:30–34.
10. Erlandsen, S.L., S.R. Hasslen, and R.D. Nelson. 1993. Detection and spatial distribution of the β_2 integrin (Mac-1) and L-selectin (LECAM-1) adherence receptors on human neutrophils by high-resolution field emission SEM. *J. Histochem. Cytochem.* 41:327–333.
11. Picker, L.J., R.A. Warnock, A.R. Burns, C.M. Doerschuk, E.L. Berg, and E.C. Butcher. 1991. The neutrophil selectin LECAM-1 presents carbohydrate ligands to the vascular selectins ELAM-1 and GMP-140. *Cell.* 66:921–933.
12. Van Ewijk, W. 1980. Immunoelectron-microscopic characterization of lymphoid microenvironments in the lymph node and thymus. *In* Blood Cells and Vessel Walls: Functional Interactions. R. Porter, M. O'Connor, and J. Whelan, editors. Excerpta Medica, New York. 71:21–37.
13. Moore, K.L., K.D. Patel, R.E. Bruehl, L. Fugang, D.A. Johnson, H.S. Lichenstein, R.D. Cummings, D.F. Bainton, and R.P. McEver. 1995. P-selectin glycoprotein ligand-1 mediates rolling of human neutrophils on P-selectin. *J. Cell Biol.* 128:661–671.
14. Berlin, C., R.F. Bargatze, U.H. von Andrian, M.C. Szabo, S.R. Hasslen, R.D. Nelson, E.L. Berg, S.L. Erlandsen, and E.C. Butcher. 1995. α4 integrins mediate lymphocyte attachment and rolling under physiologic flow. *Cell.* 80:413–422.
15. Abitorabi, M.A., R.K. Pachynski, R.E. Ferrando, M. Tidswell, and D.J. Erle. 1997. Presentation of integrins on leukocyte microvilli: a role for the extracellular domain in determining membrane localization. *J. Cell Biol.* 139:563–571.
16. von Andrian, U.H., S.R. Hasslen, R.D. Nelson, S.L. Erlandsen, and E.C. Butcher. 1995. A central role for microvillous receptor presentation in leukocyte adhesion under flow. *Cell.* 82:989–999.
17. Schmid-Schönbein, G.W., S. Usami, R. Skalak, and S. Chien. 1980. The interaction of leukocytes and erythrocytes in capillary and postcapillary vessels. *Microvasc. Res.* 19:45–70.
18. Firrell, J.C., and H.H. Lipowsky. 1989. Leukocyte margination and deformation in mesenteric venules of rat. *Am. J. Physiol.* 256:H1667–H1674.
19. Robineaux, R., and S. Bazin. 1951. Etude de la mobilité électrophorétique des leucocytes humains. *Le Sang.* 22:241–247.
20. Lichtman, M.A., and R.I. Weed. 1970. Electrophoretic mobility and N-acetyl neuraminic acid content of human nor-

mal and leukemic lymphocytes and granulocytes. *Blood*. 35: 12–22.
21. Pelikan, P., M.A. Gimbrone, and R.S. Cotran. 1979. Distribution and movement of anionic cell surface sites in cultured human vascular endothelial cells. *Atherosclerosis*. 32:69–80.
22. Mebius, R.E., and S.R. Watson. 1993. L- and E-selectin can recognize the same naturally occurring ligands on high endothelial venules. *J. Immunol*. 151:3252–3260.
23. Berg, E.L., J. Magnani, R.A. Warnock, M.K. Robinson, and E.C. Butcher. 1992. Comparison of L-selectin and E-selectin ligand specificities: the L-selectin can bind the E-selectin ligands sialyl Le^x and sialyl Le^a. *Biochem. Biophys. Res. Commun*. 184:1048–1055.
24. Kishimoto, T.K., M.A. Jutila, and E.C. Butcher. 1990. Identification of a human peripheral lymph node homing receptor: a rapidly down-regulated adhesion molecule. *Proc. Natl. Acad. Sci. USA*. 87:2244–2248.
25. Mulligan, M.S., J. Varani, M.K. Dame, C.L. Lane, C.W. Smith, D.C. Anderson, and P.A. Ward. 1991. Role of endothelial–leukocyte adhesion molecule 1 (ELAM-1) in neutrophil-mediated lung injury in rats. *J. Clin. Invest*. 88:1396–1406.
26. von Andrian, U.H., J.D. Chambers, E.L. Berg, S.A. Michie, D.A. Brown, D. Karolak, L. Ramezani, E.M. Berger, K.E. Arfors, and E.C. Butcher. 1993. L-selectin mediates neutrophil rolling in inflamed venules through sialyl $Lewis^x$-dependent and -independent recognition pathways. *Blood*. 82:182–191.
27. Zehnder, J.L., K. Hirai, M. Shatsky, J.L. McGregor, L.J. Levitt, and L.L. Leung. 1992. The cell adhesion molecule CD31 is phosphorylated after cell activation. Down-regulation of CD31 in activated T lymphocytes. *J. Biol. Chem*. 267:5243–5249.
28. Horton, R.M., H.D. Hunt, S.N. Ho, J.K. Pullen, and L.R. Pease. 1989. Engineering hybrid genes without the use of restriction enzymes: gene splicing by overlap extension. *Gene*. 77:51–59.
29. Stockton, B.M., G. Cheng, N. Manjunath, B. Ardman, and U.H. von Andrian. 1998. Negative regulation of T cell homing by CD43. *Immunity*. 8:373–381.
30. von Andrian, U.H., P. Hansell, J.D. Chambers, E.M. Berger, I.T. Filho, E.C. Butcher, and K.E. Arfors. 1992. L-selectin function is required for β_2-integrin–mediated neutrophil adhesion at physiological shear rates in vivo. *Am. J. Physiol*. 263:H1034–H1044.
31. Pries, A.R. 1988. A versatile video image analysis system for microcirculatory research. *Int. J. Microcirc. Clin. Exp*. 7:327–345.
32. Ley, K., and P. Gaehtgens. 1991. Endothelial, not hemodynamic, differences are responsible for preferential leukocyte rolling in rat mesenteric venules. *Circ. Res*. 69:1034–1041.
33. Fors, B.P., K. Goodarzi, and U.H. von Andrian. 1996. L-selectin shedding is independent of its subsurface structure and topography. *FASEB (Fed. Am. Soc. Exp. Biol.) Mtg*. A1199. (Abstr.)
34. Alon, R., S. Chen, K.D. Puri, E.B. Finger, and T.A. Springer. 1997. The kinetics of L-selectin tethers and the mechanics of selectin-mediated rolling. *J. Cell Biol*. 138: 1169–1180.
35. Ley, K., T.F. Tedder, and G.S. Kansas. 1993. L-selectin can mediate leukocyte rolling in untreated mesenteric venules in vivo independent of E- or P-selectin. *Blood*. 82:1632–1638.
36. Melder, R.J., L.L. Munn, S. Yamada, C. Ohkubo, and R.K. Jain. 1995. Selectin- and integrin-mediated T-lymphocyte rolling and arrest on TNF-α–activated endothelium: augmentation by erythrocytes. *Biophys. J*. 69:2131–2138.
37. von Andrian, U.H. 1997. A massage for the journey: keeping leukocytes soft and silent. *Proc. Natl. Acad. Sci. USA*. 94: 4825–4827.
38. De Bruyn, P.P., and Y. Cho. 1990. Structure and function of high endothelial postcapillary venules in lymphocyte circulation. *Nature*. 84:85–101.
39. Bevilacqua, M.P., S. Stengelin, M.A. Gimbrone, and B. Seed. 1989. Endothelial leukocyte adhesion molecule 1: an inducible receptor for neutrophils related to complement regulatory proteins and lectins. *Science*. 243:1160–1165.
40. Kansas, G.S., K. Ley, J.M. Munro, and T.F. Tedder. 1993. Regulation of leukocyte rolling and adhesion to high endothelial venules through the cytoplasmic domain of L-selectin. *J. Exp. Med*. 177:833–838.
41. Finger, E.B., R.E. Bruehl, D.F. Bainton, and T.A. Springer. 1996. A differential role for cell shape in neutrophil tethering and rolling on endothelial selectins under flow. *J. Immunol*. 157:5085–5096.
42. Brenner, B., E. Gulbins, K. Schlottmann, U. Koppenhoefer, G.L. Busch, B. Walzog, M. Steinhausen, K.M. Coggeshall, O. Linderkamp, and F. Lang. 1997. L-selectin activates the Ras pathway via the tyrosine kinase p56lck. *Proc. Natl. Acad. Sci. USA*. 93:15376–15381.
43. Hwang, S.T., M.S. Singer, P.A. Giblin, T.A. Yednock, K.B. Bacon, S.I. Simon, and S.D. Rosen. 1996. GlyCAM-1, a physiologic ligand for L-selectin, activates β2 integrins on naive peripheral lymphocytes. *J. Exp. Med*. 184:1343–1348.
44. Fuhlbrigge, R.C., J.D. Kieffer, D. Armerding, and T.S. Kupper. 1997. Cutaneous lymphocyte antigen is a specialized form of PSGL-1 expressed on skin-homing T cells. *Nature*. 389:978–981.
45. Steegmaier, M., E. Borges, J. Berger, H. Schwarz, and D. Vestweber. 1997. The E-selectin–ligand ESL-1 is located in the Golgi as well as on microvilli on the cell surface. *J. Cell Sci*. 110:687–694.
46. Degrendele, H.C., P. Estess, L.J. Picker, and M.H. Siegelman. 1996. CD44 and its ligand hyaluronate mediate rolling under physiologic flow: a novel lymphocyte–endothelial cell primary adhesion pathway. *J. Exp. Med*. 183:1119–1130.
47. Steegmaier, M., A. Levinovitz, S. Isenmann, E. Borges, M. Lenter, H.P. Kocher, B. Kleuser, and D. Vestweber. 1995. The E-selectin–ligand ESL-1 is a variant of a receptor for fibroblast growth factor. *Nature*. 373:615–620.
48. Kansas, G.S. 1996. Selectins and their ligands: current concepts and controversies. *Blood*. 88:3259–3287.
49. Puri, K.D., E.B. Finger, and T.A. Springer. 1997. The faster kinetics of L-selectin than of E-selectin and P-selectin rolling at comparable binding strength. *J. Immunol*. 158:405–413.
50. Zhao, Y., S. Chien, and R. Skalak. 1995. A stochastic model of leukocyte rolling. *Biophys. J*. 69:1309–1320.
51. Hammer, D.A., and S.M. Apte. 1992. Simulation of cell rolling and adhesion on surfaces in shear flow: general results and analysis of selectin-mediated neutrophil adhesion. *Biophys. J*. 63:35–57.